Desalination and Water Treatment
www.deswater.com

doi: 10.5004/dwt.2020.26465

208 (2020) 104–109
December

Development of carbon nanotube membranes for dissolved gases removal as seawater pretreatment

Bhadrachari Garudachari*, Ali Al-Odwani, Rajesha Kumar Alambi, Mohammad Al-Tabtabaei, Y. Al-Foudari

Water Research Center, Kuwait Institute for Scientific Research, P.O. Box: 24885, Safat 13109, Kuwait, Tel. +965 98724398; emails: bgarudachari@kisr.edu.kw/garuda.achar@gmail.com (B. Garudachari), aodwani@kisr.edu.kw (A. Al-Odwani), ralambi@kisr.edu.kw (R.K. Alambi), mtabtaba@kisr.edu.kw (M. Al-Tabtabaei), yfoudari@kisr.edu.kw (Y. Al-Foudari)

Received 1 December 2019; Accepted 17 August 2020

ABSTRACT

The removal of dissolved gases such as oxygen from seawater is one of the primary process applied in desalination industries. The effective degasification of dissolved gases remains a challenge in the desalination industry due to several reasons such as removal efficiency, performance, gas selectivity, and others. This paper describes the fabrication, characterization, and degasification performance study of carbon nanotube/polyvinyl chloride (CNT/PVC) nanocomposite membranes. The CNT/PVC nanocomposite membranes were fabricated by immersion precipitation method at 0.01, 0.25, and 0.5 wt.% CNT concentrations in the casting solution. The physicochemical properties of fabricated membranes were studied by Fourier transform infrared spectroscopy (FTIR), field emission scanning electron microscopy (FESEM), atomic force microscopy (AFM), contact angle (CA), water uptake, and liquid entry pressure (LEP). The FTIR analysis confirmed the proper dispersion of CNT throughout the membrane. The values of CA, water uptake, and LEP decreased with the increase of CNT concentration in the membrane matrix. The FESEM and AFM studies showed an increase in macrovoid structure and a decrease in surface roughness with increased CNT concentration. The newly fabricated membranes showed excellent degasification performance under the prevalent conditions of the desalination process.

Keywords: Carbon nanotube/polyvinyl chloride membrane; Degasification; Flux; Contact angle; Liquid entry pressure

1. Introduction

The corrosion is one of the major problem in the desalination industries due to the intake of high saline feed water. High saline feed water easily corrodes the pipelines, desalination boilers, instruments which are in direct contact with feed water. Therefore, desalination industries require high standard materials and regular maintenance. There are number of emerging technologies to solve the corrosion problems in desalination industries. One of the economically feasible technology is removal of dissolved oxygen (DO) from boiler feed water to protect the boiler from corrosion [1,2]. The dissolved oxygen (DO) in feed water results in boiler or steel pipe damage by developing metal oxide on the surface. The most common dissolved gases are oxygen, carbon dioxide, and hydrogen sulfide [3–5]. The current methods used for DO removal are either mechanical or chemical treatments. In the chemical treatment method, hydrazine is used as a chemical for converting DO into water and nitrogen. However, hydrazine has limitations such as slow reaction rate, undesired byproduct, and intrinsic harmful property (toxicity). On the other hand, mechanical processes have inherent drawbacks as they are complex, costly, and energy intense [6]. New membrane-based technologies known as membrane contactors

* Corresponding author.

1944-3994/1944-3986 © 2020 Desalination Publications. All rights reserved.

(MCs) can offer far more reliable option for removal of dissolved gases from feedwaters [5,7–9]. The membrane degasification is a liquid–gas separation process using membrane as a separation barrier. In this process, the membrane is hydrophobic and allows only gas component to diffuse through the membrane. The major challenge in membrane degasification is to develop a membrane with a lower energy barrier between liquid and gas separation. Zhang et al. [10] reported that the carbon nanotube (CNT) membrane with CNT having average pore size of 1.2 nm showed high gas (oxygen) permeance. The high oxygen permeance of CNT attracted researchers to develop a CNT membrane for degasification in the desalination industries [10]. Over the last decade, membranes for degasification have developed significantly; today the technology is commercially available for degasification of boiler feed water and desalination units such as reverse osmosis (RO) [11]. The advantages of recent MCs compared with other gas removal processes are higher efficiency, chemically free, more compact, smaller footprint, and lighter weight which reduces capital investment. Furthermore, it is flexible and easy to scale up [12]. In the degasification process, hydrophobic membrane showed promising effects in consumption of low energy and high gas separation efficiency [13,14], and this will eventually lead to lower boiler, pipeline corrosion, and low maintenance or instrument replacement charges in the water treatment process. Considering the advantages of hydrophobic polymer membranes in the degasification process, CNT nanoparticle was incorporated in polyvinylchloride (PVC) polymer membranes. The main objective of this study was to fabricate high-performance CNT incorporated PVC membranes for the DO removal application and to enhance the DO removal performance for boiler feed water in the desalination. In the present study, CNT nanoparticle incorporated PVC polymer membranes were fabricated using diffusion induced phase separation method (DIPS). All the newly fabricated membranes were characterized using contact angle (CA) goniometer, liquid entry pressure (LEP) test, field emission scanning electron microscopy (FESEM), and atomic force microscopy (AFM). Fabricated membranes showed increasing trend of oxygen flux with an increase of CNT concentration in the membrane and increased oxygen removal efficiency with increase of vacuum level.

2. Experimental

2.1. Materials

All the chemicals, and reagents required for the laboratory experiments, calibration, and analysis were purchased from international suppliers and used without any further purification. These include low molecular weight polyvinyl chloride (PVC; CAS: 9002-86-2), CNT, dimethylformamide (DMF), and polyethylene glycol 400 (PEG 400). Deionized (DI) water from Millipore Milli-Q-Direct was used for all the experiments.

2.2. Fabrication of CNT/PVC nanocomposite membranes

Flat sheet CNT/PVC nanocomposite membranes were fabricated by immersion precipitation method using 0.01, 0.25, and 0.5 wt.% CNT in the casting solution. The weight percentage of CNT was selected based on the literature study of CNT based membrane and trial and error methods. In brief, precisely calculated amounts of PVC and PEG 400 were added to the desired volume of DMF solvent and were subjected to magnetic stirring for 10 h at 60°C. After complete dissolution of the polymer, calculated amount CNT was added and continued stirring for another 8 h at 60°C and sonicated for 15 min. The homogeneous solution was cast using Doctor's blade and gently immersed in the coagulation bath. The similar procedure was employed for the preparation of all CNT/PVC membrane with different CNT composition. The overview of the composition is tabulated in Table 1.

2.3. Characterization of CNT/PVC membrane

All the fabricated membranes (four concentration of CNT: 4 × triplicate = total 12 samples) were characterized by using highly sophisticated. ALPHA-Fourier transform infrared spectroscopy (FTIR) spectrophotometer (Bruker: 1228 4854, Germany) was used to characterize the chemical structure polymer and CNT nanoparticle. The FTIR scanning was taken with 64 scans in the range of 4,000–400 cm^{-1}. The contact angles were measured using Goniometer. Keysight 8500 FESEM was used to study the surface and cross-sectional morphology of the membranes. The membrane surface topological features were analyzed using nano-observer AFM instrument by scanning the membrane 10 μm × 10 μm dimensions.

2.4. Dissolved oxygen removal application

Newly fabricated CNT/PVC contactors (four concentration of CNT: 4 × triplicate = total 12 samples) performance analysis was carried out by laboratory scale degasification unit as shown in Fig. 1. In brief, water was circulated through the one side of the module with controlled DO concentration and vacuum was applied on the other side of the module in the degassing process. DO concentration in water

Table 1
Composition of different CNT/PVC membranes casting solution

Sl. No	Membrane code	PVC (wt.%)	DMF (wt.%)	CNT (wt.%)	PEG 400 (wt.%)
1	MC 01	16	81	0.00	3.0
2	MC 02	16	80.9	0.10	3.0
3	MC 03	16	80.7	0.25	3.0
4	MC 04	16	80.5	0.50	3.0

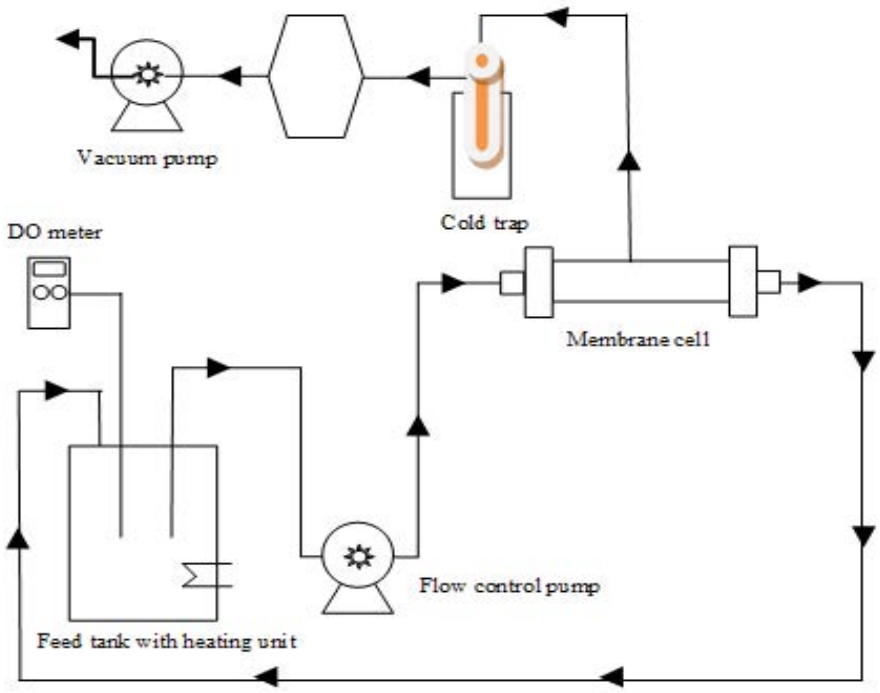

Fig. 1. Schematic representation of degasification apparatus for DO removal.

was measured every hour using DO meter (HQ440d). The oxygen flux (J_0), and water flux (J_w) was calculated according to the following equations [14]:

Permeate flux of DO (mg/m² h):

$$J_0 = \frac{Q_0}{A \times \Delta T} \quad (1)$$

Permeate water flux (L/m²h):

$$J_w = \frac{Q_w}{A \times \Delta T} \quad (2)$$

where Q_0 is oxygen removed from feed water (mg), Q_w is colllected water in cold trap (L), ΔT is experimental duration (h), A is membrane area (m²) [14]. Perperformance study was conducted in triplicate for each membrane and mean value is reported.

3. Results and discussion

3.1. FTIR analysis

The FTIR spectra of CNT/PVC nanocomposite membranes show the presence of signature peaks corresponding to CNT and PVC polymer. Fig. 2 clearly indicates the peaks at 2,918 and 2,855 cm^{-1} corresponds to the C–H stretching of PVC polymer. The phase vibration band of CH_2 has appeared at 1,429 cm^{-1} and C–Cl stretching peak appeared at 753 cm^{-1}. The presence of a broad peak at 3,354 cm^{-1} corresponds to the O–H and C=C of hexagonal carbon appeared at 1,587–1,648 cm^{-1} confirms the CNT incorporation in the prepared membrane [15–17].

3.2. Membrane morphology

3.2.1. FESEM analysis

The gas selectivity and degasification properties of the membranes are strongly depending on the morphology of the membrane. The FESEM is the prominent technique to study the morphological variation of newly developed CNT/PVC membranes. Fig. 3 shows the magnified surface image of MC 01 and MC 04 membrane at 10,000; 15,000; and 20,000 magnification. The increase in porosity and uniform pore distribution with the increase in CNT concentration in the membrane casting solution is clearly shown in Fig. 3 cross-section FESEM images of membranes exhibited asymmetric characteristics with a dense top layer followed by the porous support layer. The increase of CNT concentration in the PVC casting solution resulted in an increase of macrovoid structures and pore size. This is mainly due to the addition of CNT in the casting solution significantly alters the viscosity of the casting solution resulted in the changes in the morphological features of the membrane.

3.2.2. AFM analysis

AFM study showed slight decrease in surface roughness as CNT concentration is increase from 0.1 to 0.25 wt.%, and further increase of CNT concentration increased the surface roughness. In low concentration, due to the low electrostatic interaction between the CNTs, they are regularly arranged in the membrane and reduced the surface roughness. At high concentration due to agglomeration and increase of pore size increased surface roughness [18,19]. The lowest average roughness recorded was 497 nm for 0.25 wt.% CNT/PVC membrane and highest recorded was

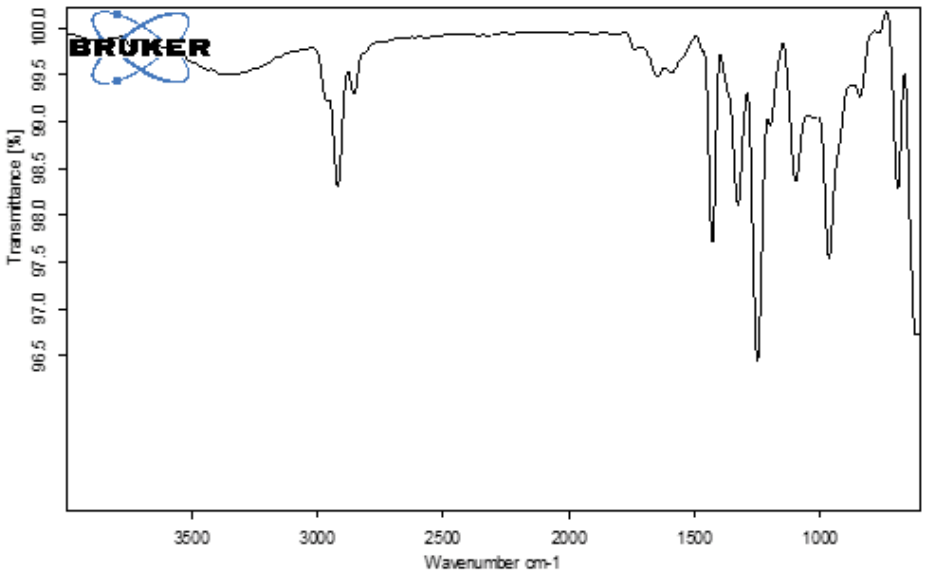

Fig. 2. FTIR spectrum of CNT/PVC membrane.

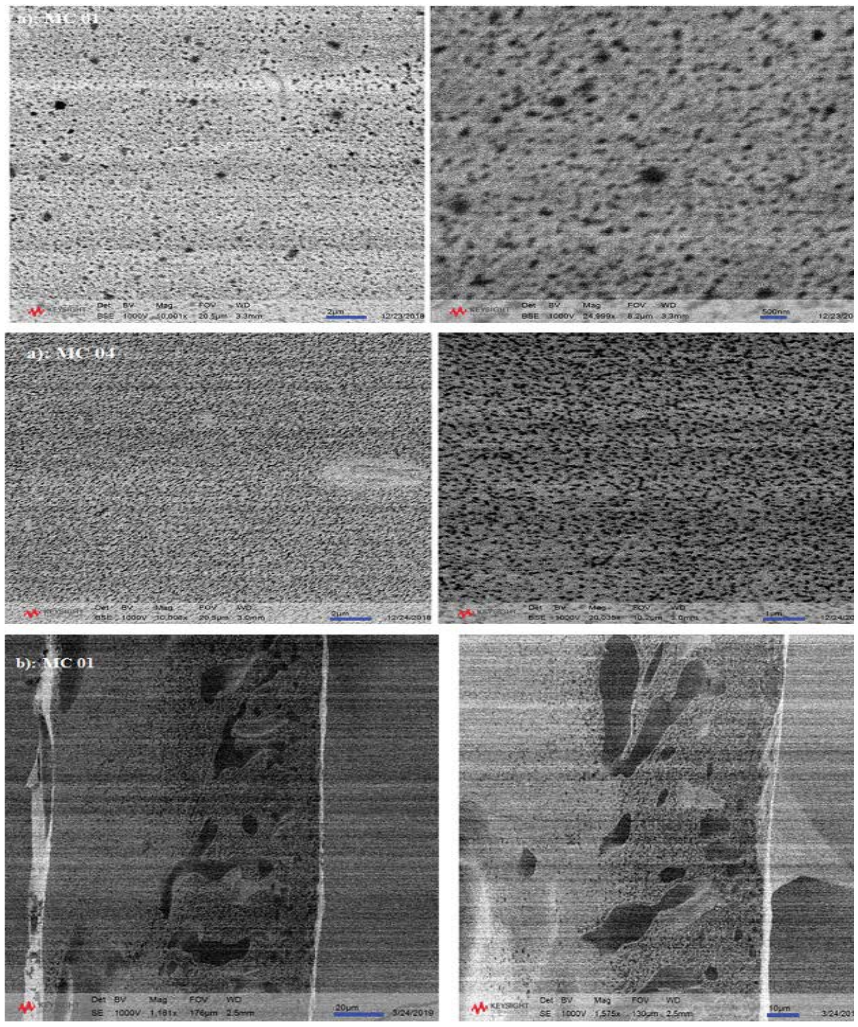

Fig. 3. (a and b) Magnified surface image and cross-sectional FESEM images of MC 01and MC 04 membranes.

761 nm for 0.5 wt.% CNT/PVC. The surface AFM images of the CNT/PVC membranes with different concentrations of CNT are shown in Fig. 4.

3.3. Analysis of water contact angle, water uptake, and liquid entry pressure

The water uptake and CA study revealed that increase of CNT weight percentage in the membrane matrix decreases water uptake and increases CA. The increased percentage of CNT shows an increasing trend of CA in the order of MC 01 < MC 02 < MC 03 < MC 04. The increase in CA with an increase of CNT percentage in the membrane matrix is due to the hydrophobic nature of CNT. The CA increased from 71° for PVC to 77° for 0.5 weight percentage CNT incorporated PVC membrane. The hydrophobic nature of CNT/PVC membrane also supported the decrease in the water uptake capacity by increasing the concentration of CNT. The increase in CNT concentration in the membrane matrix decreased the LEP value and this is mainly due to the increase of pore size. The water contact angle, water uptake, and liquid entry pressure values for the CNT/PVC membranes are presented in Table 2.

3.4. Membrane degasification performances

The degasification performance of the CNT/PVC membrane is mainly depending on the nature of feed solution, structural properties, and chemical behavior of membrane. Preliminary degasification tests were conducted for all the membranes using a laboratory scale instrument as shown in Fig. 1. Laboratory results showed that the membrane with 0.5 weight percentage of CNT showed highest oxygen flux compared with other membranes as shown in Fig. 5a. The highest oxygen flux was 800 mg/m^2 h and corresponding water flux was 15.5 L/m^2 h. The order of oxygen flux is MC 04 > MC 03 > MC 02 > MC 01. This increasing trend of oxygen flux with an increase of CNT concentration in the membrane is due to the additional porous structure from CNT and morphological changes of the membrane. Fig. 5b shows the effect of operating vacuum on oxygen removal efficiency of MC 04 membrane. Oxygen removal efficiency increased with an increase of vacuum level from –50 to –90 kPa. The increase of oxygen flux with an increase in the vacuum is due to the increased chemical potential difference between feed and permeate side which is created by applied vacuum [1,14]. Deeper vacuum level creates the drop-in oxygen partial pressure on the downstream of the degasification cell results the higher DO efficiency.

4. Conclusion

The CNT incorporated PVC membranes were fabricated by phase inversion method. The fabricated membranes were characterized using FTIR, AFM, FESEM, LEP, and contact angle goniometer. The FTIR spectra of CNT/PVC nanocomposite membranes show the presence of signature peaks corresponding to CNT and PVC polymer. The CA increased with the increase in CNT concentration in the CNT/PVC nanocomposite membrane, whereas, the water uptake and

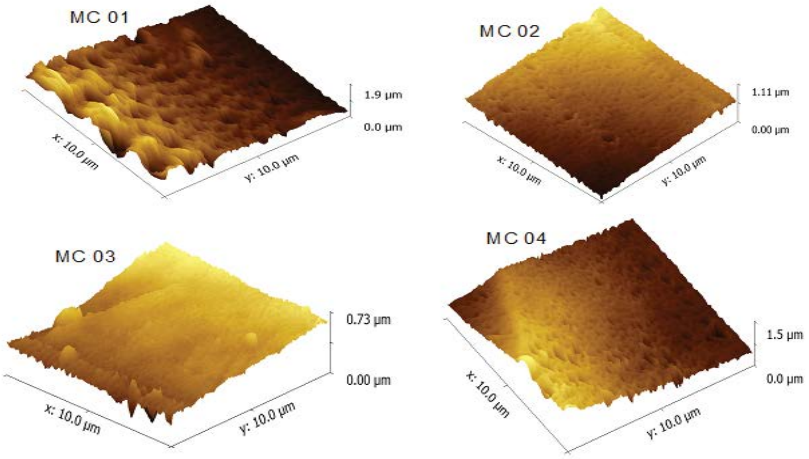

Fig. 4. Three-dimensional AFM images of MC 01, MC 02, MC 03, and MC 04 membranes.

Table 2
Water contact angle (CA), water uptake, and liquid entry pressure (LEP) values of CNT/PVC membranes

Sl. No	Membrane code	CA (°)	Water uptake (%)	LEP (bar)
1	MC 01	71.07	13.92	5.86
2	MC 02	73.16	3.84	4.82
3	MC 03	74.04	2.36	4.48
4	MC 04	77.46	2.30	3.79

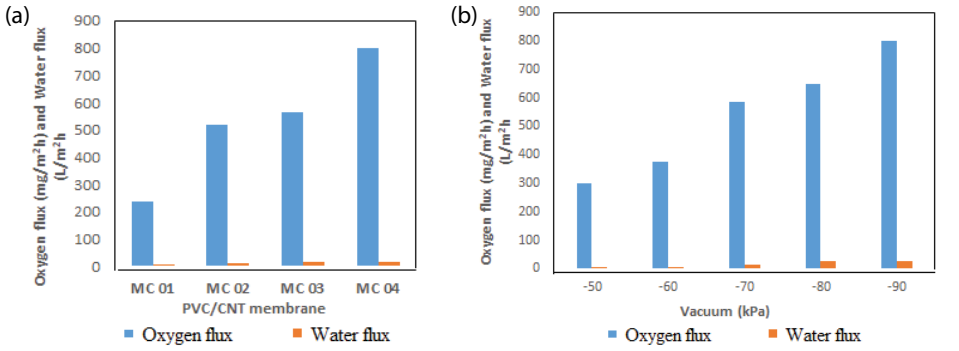

vacuum: -90 kPa, flow rate: 30L/h, initial concentration of DO: 9 mg/L, temperature: 25 ℃.

flow rate: 30L/h, initial concentration of DO: 9 mg/L, temperature: 25 ℃,

Fig. 5. Performance study. Effect of (a) CNT content and (b) vacuum on degasification performance.

LEP decreased with the increase of CNT concentration in the CNT/PVC nanocomposite membrane. The cross-sectional FESEM image and three-dimensional AFM images showed the change in morphology and surface roughness properties of resultant CNT/PVC membrane due to the interaction of CNT and PVC polymer in the membrane casting process. The highest CA observed was 77° for 0.5 wt.% CNT/PVC membranes and the corresponding LEP was 3.79 bar. The laboratory scale degasification experiments showed an increase of degasification performance with the increase of vacuum level. The membrane with 0.5 wt.% of CNT in the membrane matrix showed improved DO removal capacity and can be a promising candidate for the dissolved gas removal applications in the desalination processes.

Acknowledgment

Authors are thankful to the Kuwait Institute for Scientific Research (KISR) for funding and supporting the implementation of this research work.

References

[1] J. Shao, H. Liu, Y. He, Boiler feed water deoxygenation using hollow fiber membrane contactor, Desalination, 234 (2008) 370–377.
[2] P. Costa, A. Ferro, E. Ghiazza, B. Bosio, Seawater deaeration at very low steam flow rates in the stripping section, Desalination, 201 (2006) 306–314.
[3] E. Schaschl, G.A. Marsh, The effect of dissolved oxygen on corrosion of steel and on current required for cathodic protection, Corrosion, 13 (1956) 35–43.
[4] I. Al-Mutaz, F.A. Aleem, A. Al-arifi, Corrosion and Scale Formation Problems in Water Systems, The 2011 International Conference on Water, Energy, and the Environment, American University of Sharjah, Sharjah, UAE, 2011, pp. 1–6. Available at: https://www.researchgate.net/publication/278486524_Corrosion_and_Scale_Formation_Problems_in_Water_Systems
[5] M. Al-Tabtabaei, A. Al-Odwani, A. Al-Haji, A. Al-Sairafi, A. Al-Mesri, Assessment of The Viability and Efficiency of Membrane Contactors for Deaeration – Bench-Scale Study, Kuwait Institute for Scientific Research, Final Report WT030K, 2016, pp. 1–282.
[6] I.B. Butler, A. Martin, M.A. Schoonen, D.T. Rickard, Removal of dissolved oxygen from water: a comparison of four common techniques, Talanta, 41 (1994) 211–215.
[7] O.S. Degenhardt, B. Waters, A. Rebelo-Cameirao, A. Meyer, H. Brunner, N.P. Toltl, Comparison of the effectiveness of various deaeration techniques, Dissolution Technol., (2004) 6–10, doi: 10.14227/DT110104P6.
[8] N. Ghasem, Modeling and simulation of CO_2 absorption enhancement in hollow-fiber membrane contactors using CNT–water-based nanofluids, J. Membr. Sci. Res., 5 (2019) 295–302.
[9] Y. Xu, C. Malde, R. Wang, Correlating physicochemical properties of commercial hollow fiber membranes with CO_2 absorption performance in gas-liquid membrane contactor, J. Membr. Sci. Res., 6 (2019) 30–39.
[10] L. Zhang, B. Zhao, C. Jiang, J. Yang, G. Zheng, Preparation and transport performances of high-density, aligned carbon nanotube membranes, Nanoscale Res. Lett., 266 (2015) 2–8.
[11] Membrana-Charlotte, Liqui-Cel® Membrane Contactor Technology Being Evaluated for Dissolved Gas Removal from Water in Many Hydrocarbon Processes Liqui-Cel Membrane contactors, 2012. Available at: https://mailgooglecom/mail/u/0/?tab=wm#inbox
[12] R. Tesser, A. Bottino, G. Capannelli, F. Montagnaro, S. Vitolo, M.D. Serio, E. Santacesaria, Advantages in the use of membrane contactors for the study of gas-liquid and gas-liquid-solid reactions, Ind. Eng. Chem. Res., 44 (2005) 9451–9460.
[13] A. Mansourizadeh, A.F. Ismail, Hollow fiber gas–liquid membrane contactors for acid gas capture: a review, J. Hazard. Mater., 171 (2009) 38–53.
[14] T. Li, P. Yu, Y. Luo, Deoxygenation performance of polydimethylsiloxane mixed-matrix membranes for dissolved oxygen removal from water, J. Appl. Polym. Sci., 132 (2015) 1–9, doi: 101002/APP41350.
[15] R. Yudianti, H. Onggo, S. Sudirman, Y. Saito, T. Iwata, J.-I. Azuma, Analysis of functional group sited on multi-wall carbon nanotube surface, Open Mater. Sci. J., 5 (2011) 242–247.
[16] I.S. Elashmawi, N.S. AIatawia, N.H. Elsayed, Preparation and characterization of polymer nanocomposites based on PVDF/PVC doped with graphene nanoparticles, Results Phys., 7 (2017) 636–640.
[17] A.J. Clancy, D.B. Anthony, S.J. Fisher, H.S. Leese, C.S. Roberts, M.S.P. Shaffer, Reductive dissolution of supergrowth carbon nanotubes for tougher nanocomposites by reactive coagulation spinning, Nanoscale, 9 (2017) 8764–8773.
[18] V. Vatanpoura, S.S. Madaenia, R. Moradianb, S. Zinadinia, B. Astinchap, Fabrication and characterization of novel antifouling nanofiltration membrane prepared from oxidized multiwalled carbon nanotube/polyethersulfone nanocomposite, J. Membr. Sci., 375 (2011) 284–294.
[19] P. Daraei, S.S. Madaeni, N. Ghaemi, H.A. Monfared, M.A. Khadivi, Fabrication of PES nanofiltration membrane by simultaneous use of multi-walled carbon nanotube and surface graft polymerization method: comparison of MWCNT and PAA modified MWCNT, Sep. Purif. Technol., 104 (2013) 32–44.